

Second Harmonic signal detection on Poly [μ_2 -L-alanine- μ_3 -nitratosodium (I)] crystals.

E. Gallegos-Loya, E. Álvarez Ramos, E. Regalado, A. Duarte-Moller

Abstract

Crystals of poly (L-alanine sodium nitrate) have been grown by the slow evaporation at room temperature method. Crystal sizes of 500mm and 10 mm were obtained. UV-vis spectrum shows a wide transparent window where lack of absorption around the 532 nm. By other hand the FTIR analysis displays its functional groups corresponding to the alanine. The Single Crystal Diffraction experiment was carried out in order to determine the atomic structure and its lattice parameter. Finally as a first time the second harmonic generation was measured by using a variant of the Kurtz Perry method. The efficiency was plotted and discussed.

Keywords: L. alanine, SHG, NLO, semiorganic, alanine

Introduction

In the modern world, the development of science in many areas has been achieved through the growth of single crystals. Nonlinear optical (NLO) materials have been studied extensively for their possible applications in various fields, are expected to play a major role in the technology of photonics like telecommunication, optical computing, optical data storage and optical information processing. [1, 2]

The generation of coherent blue light through second harmonic generation (SHG) from near infrared (NIR) laser sources is an important technological problem that has attracted much attention in the last few years. [2] Coherent blue and green light are

important for many applications such as display, high-resolution printing, and signal processing. [3].

Some organic compounds exhibit large NLO response, in many cases, orders of magnitude larger than widely known inorganic materials. They also offer the flexibility of molecular design and the promise of virtually an unlimited number of crystalline structures. [1] A number of such crystals, especially from the amino acid family, have recently been reported [4–8]. Some crystals of the amino acids with simple inorganic salts appear to be promising materials for optical second harmonic generation (SHG). [9].

The aminoacids display specific features of interest, such as (i) molecular chirality, which secures acentric crystallographic structures; (ii) absence of strongly conjugated bonds, leading to wide transparency ranges in the visible and UV spectral regions; (iii) zwitterionic nature of the molecule, which favours crystal hardness. [2] Further to that, aminoacids can be used (iv) as chiral auxiliaries for nitro-aromatics and other donor–acceptor molecules with large hyperpolarizabilities and (v) as a basis for synthesizing organic–inorganic compounds [10].

A series of studies on semiorganic amino acid compounds such as L-arginine phosphate (LAP), L-arginine hydrobromide (L-AHBr), L-histidine tetrafluoroborate (L-HFB), [11] L-arginine hydrochloride (L-AHCl), [12] L-alanine acetate (LAA), [13] and glycine sodium nitrate (GSN) [14] as potential NLO crystals have been reported.

L-Alanine is an amino acid, and it forms a number of complexes on reaction with inorganic acid and salts to produce an outstanding material for NLO applications. [11] The compound was first crystallized by Bernl and later by Simpson et al. It belongs to

the orthorhombic crystal system (space group P212121) with a molecular weight of 89.09 and has a melting point of 297 °C. [1]

The compound, Poly[μ 2-L-alanine- μ 3-nitratosodium (I)] , [Na(NO₃)(C₃H₇NO₂)]_n[15] was obtained as the product of an attempted reaction of sodium nitrate and the amino acid L-alanine in aqueous solution. In the present investigation, single crystals were grown and characterized by single crystal X-ray diffraction. Fourier transform infrared (FTIR) spectroscopic studies, thermo gravimetric analysis (TGA/DSC), UV–Vis–NIR spectral analysis and second harmonic generation (SHG).

Polyoxometalates (POMs) can be considered as oligomeric aggregates of metal cations, bridged by oxide anions that form by self-assembly processes (Rhule et al., 1998). There are two generic families of POMs, the isopolyoxometalates, that contain only d⁰ metal cations and oxide anions and the heteropolyoxometalates, that contain one or more *p*-, *d*-, or *f*-block heteroatoms in addition to the other ions (Pope, 1983; Rhule et al., 1998).

The medicinal features of these compounds cover a variety of important biological activities, such as the inhibition of specific enzymes or antiviral and antitumor activity (Pope and Mueller, 1994; Rhule et al., 1998). When used in combination with β -lactam antibiotics, polyoxotungstates enhance the antibiotic effectiveness against otherwise resistant strains of bacteria (Yamase et al., 1996). The heptamolybdate, [NH₃Pri]₆[Mo₇O₂₄]₆·3H₂O had shown a potent in vivo antitumor activity (Fujita, et al., 1992), which has been explained by repeated redox cycles of [Mo₇O₂₄]₆⁻ in the tumor cells (Yamase, 1993).

The biomedical investigations of polyoxomolybdates containing amino acids or even peptides (Yamase et al., 1999) have been focused upon finding polyoxomolybdates with both improved activity against cancer and clinical safety profiles.

The reported structure $\text{Na}(\text{NO}_3)\text{C}_3\text{H}_7\text{NO}_2$ was obtained unintentionally as the product of an attempted reaction of sodium molybdate in aqueous solution and the amino acid L-alanine, in order to obtain a γ type octamolybdate, coordinated by Lalanine $\text{Na}_4[\text{Mo}_8\text{O}_{26}(\text{ala})_2] \cdot 18\text{H}_2\text{O}$ (Cindrić et al., 2006). In contrast to *Cindrić et al.*, L-alanine was used instead of *D,L*-alanine.

Problem Formulation

Crystals of p-LASN are potentially important for technological applications, however there is not evidence about its non-linear optical response.

Síntesis and Growth of Poly[μ_2 -L-alanine- μ_3 -nitrate-sodium (I)].

The title compound, $[\text{Na}(\text{NO}_3)(\text{C}_3\text{H}_7\text{NO}_2)]_n$, was obtained unintentionally by Kristof Van Hecke [15] as the product of an attempted reaction of sodium molybdate in aqueous solution and the amino acid lalanine (ala), in order to obtain a γ -type octamolybdate, $\text{Na}_4[\text{Mo}_8\text{O}_{26}(\text{ala})_2] \cdot 18\text{H}_2\text{O}$, coordinated by l-alanine.

The coordination geometry around the Na atom can be considered as trigonal-bipyramidal, with three bidentate nitrate anions coordinating through their O atoms and two l-alanine molecules each coordinating through one carboxylate O atom.

The crystals obtained during the development of this work were grown by slow evaporation technique at room temperature in an aqueous solution. The reactive commercially available Lalanine $\text{C}_3\text{H}_7\text{NO}_2$ with stoichiometry Sigma-Aldrich lab with

98% purity and molecular weight 89.09 g/mol, and sodium nitrate, NaNO₃ stoichiometry Sigma-Aldrich lab with 99.9% purity and molecular weight 84.99 g/mol were used. For the development of this work samples were prepared 1:1 molar ratio in distilled water and constant agitation for 35 min and and temperature of 60°C. Evaporation of the Lalanine sodium nitrate solution at room temperature was of 45 days.

Problem solution

In order to obtain the physical properties of the Poly[μ₂-L-alanine-μ₃-nitrate-sodium (I)], p-LASN, crystals, an exhaustive characterization was developed as follows:

Optical microscopy

Fig. 1. Shows a photograph of the single crystal obtained after the low evaporation of the aqueous solution.



Fig. 1. Picture of a single crystal of the p-LASN.

X-Ray powder diffraction

The XRD data was collected using a X-PERT Phillips diffractometer with CuKα ($\lambda=1.540598 \text{ \AA}$), step of 0.05° and 2θ scanning between 10 and 60° . Finally, the samples were powders of crystals.

Fig. 2 shows the X-Ray diffraction pattern. Like other characterizations, the p-LASN, the pure Lalanine and the pure Sodium Nitrate are shown together.

Within the graph appear the main peaks taken from database information of the L-alanine, that is a Monoclinic crystal and spatial group P21/n. This crystal structure and spatial group are found in the L- Argininum Dinitrate [15] and Lithium pnitrophenolate [18].

About the p-LASN, a non-centrosymmetric structure was expected to be obtained. The options to have this kind of symmetry are the crystal systems Triclinic, Monoclinic and Orthorhombic. Two of them can be shown on the crystals with single L-alanine and Sodium Nitrate with good agreement with literature.

As we can observe there is a close similitude between both spectra, however some lines around $2\theta = 19^\circ$, 23.3° and 27.39° may establish the difference.

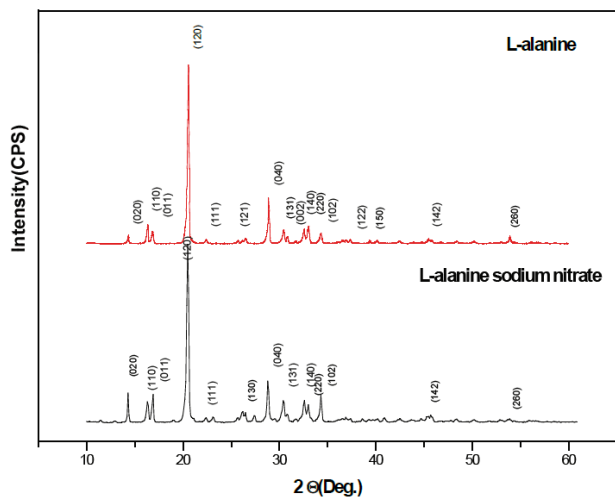


Fig. 2. Powder X-ray diffraction pattern of Poly[μ_2 -L-alanine- μ_3 -nitrate-sodium (I)] and the L-alanine reactive.

Single crystal Diffraction characterization

The right technique used to determine the structural information with good agreement is single crystal diffraction.

For this experiment a single crystal of L-alanine sodium nitrate measuring approximately 0.3 x 0.1 x 0.1 mm was mounted on a Bruker Kappa APEXII DUO diffractometer. With the crystal temperature at 298K a short set of 36 frames were collected in order to determine the unit cell. From these 36 frames were harvested 100 reflections which were used to index and refine the unit cell as:

$$a = 5.388(9) \text{ \AA}, b = 9.315(15) \text{ \AA}, c = 13.63(2) \text{ \AA}, \\ \alpha = \beta = \gamma = 90^\circ$$

This unit cell was used to search the Cambridge Structural Database¹ (version 5.30 plus four updates). A positive match was found to the paper K. Van Hecke, E. Cartuyvels, T. N. Parac-Vogt, C. Gorller-Walrand, and L. Van Meervelt. Poly[μ_2 -L-alanine- μ_3 -nitrate-sodium(I)] [15].

The authors describe the structure as follows: The asymmetric unit consists of one sodium and one nitrate ion and one L-alanine molecule. The coordination geometry around the sodium atom can be considered as trigonal bipyramidal, with three bidentate nitrate anions coordinating through their oxygen atoms and two L-alanine molecules, each coordinating through one carboxyl oxygen atom (Figure 3,4).

Three nitrate anions are bidentate coordinating to the sodium atom (2.612 (2)–2.771 (2) Å), forming one plane, parallel with the (110) plane. The third nitrate oxygen atoms are coordinating to other symmetry equivalent sodium atoms, extending the plane formed. Almost perpendicular to this plane, two L-alanine molecules are

coordinating to the sodium atom, each through one carboxyl oxygen atom (2.3651 (16) and 2.3891 (17) Å). The other carboxyl oxygen atoms are coordinated to sodium atoms in the planes above and beneath, respectively. Hence, infinite planes parallel with (110) are formed by the nitrate anions and the sodium atoms and these are perpendicularly linked to each other by Lalanine molecules (Figure 3).

Intermolecular hydrogen bonds are observed between N1(H1A)···O(1)[1/2 + x, -1/2 - y, 2 - z] (1.92 (4) Å), N1(H1B)···O(5)[1/2 + x, 1/2 - y, 2 - z] (2.10 (3) Å) and N1(H1C)···O(2)[1 + x, y, z] (1.87 (4) Å) and an intramolecular hydrogen bond is found for N1(H1B)···O(2) (2.44 (3) Å).

The authors report the structure shown in Fig. 3. This one represents the coordination geometry of the Poly[μ_2 -L-alanine- μ_3 -nitrate-sodium (I)]. As same way, Fig. 4 shows the packing diagram of the p-LASN.

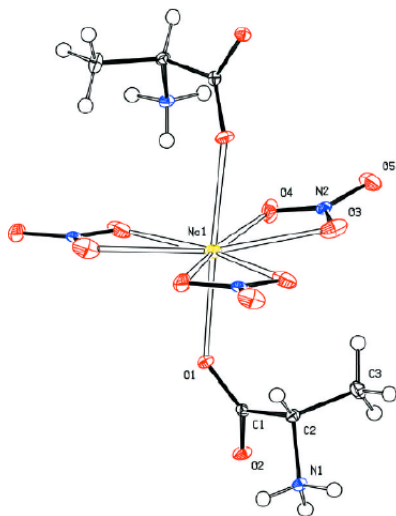


Fig. 3. Coordination geometry of the Poly[μ_2 -L-alanine- μ_3 -nitrate-sodium (I)] obtained by using single crystal diffraction.

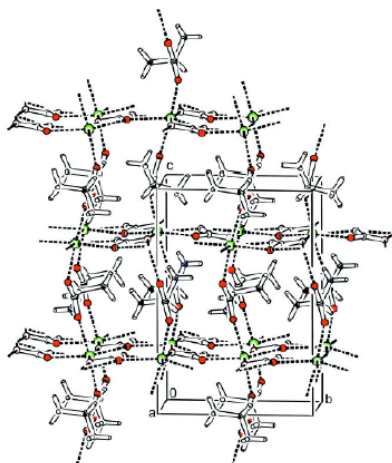


Fig. 4. Packing diagram of the Poly[μ_2 -L-alanine- μ_3 -nitrato-sodium (I)].

Additional data can be extracted from [15]. However, we display the supplementary data for the obtained structure.

Fractional atomic coordinates and isotropic or equivalent isotropic displacement parameters (\AA^2)

	x	y	z	U_{eq}^{iso}/U_{eq}
C1	0.6356 (4)	1.05721 (19)	-0.00853 (15)	0.0078 (4)
C2	0.3525 (4)	1.0453 (2)	0.00305 (15)	0.0090 (4)
C3	0.2757 (4)	0.8870 (2)	0.02082 (14)	0.0136 (4)
H2	0.300 (5)	1.109 (3)	0.0538 (19)	0.016*
H1A	0.247 (7)	1.201 (3)	-0.0929 (19)	0.020*
H3A	0.322 (5)	0.825 (3)	-0.033 (2)	0.020*
H1B	0.287 (6)	1.064 (3)	-0.140 (2)	0.020*
H1B	0.095 (6)	0.881 (3)	0.028 (2)	0.020*
H1C	0.062 (6)	1.080 (3)	-0.087 (2)	0.020*
H3C	0.348 (6)	0.841 (3)	0.082 (2)	0.020*
N1	0.2284 (4)	1.10123 (18)	-0.08786 (11)	0.0082 (3)
N2	0.7554 (4)	0.71413 (16)	0.24472 (10)	0.0087 (3)
Na1	0.75451 (17)	1.04449 (8)	0.23836 (5)	0.0127 (3)
O1	0.7615 (3)	1.09249 (14)	0.06664 (8)	0.0097 (3)
O2	0.7253 (3)	1.02859 (15)	-0.09235 (10)	0.0122 (3)
O3	0.5568 (3)	0.7841 (2)	0.24054 (13)	0.0209 (4)
O4	0.9608 (3)	0.7753 (2)	0.23456 (13)	0.0201 (4)
O5	0.7487 (4)	0.57822 (15)	0.26006 (9)	0.0211 (4)

Atomic displacement parameters (\AA^2)

	U^{11}	U^{22}	U^{33}	U^{12}	U^{13}	U^{23}
C1	0.0083 (9)	0.0061 (9)	0.0090 (9)	0.0009 (7)	-0.0015 (8)	0.0025 (7)
C2	0.0072 (9)	0.0125 (9)	0.0072 (9)	-0.0007 (8)	0.0004 (7)	-0.0005 (8)
C3	0.0106 (10)	0.0135 (9)	0.0166 (10)	-0.0021 (10)	0.0000 (9)	0.0047 (7)
N1	0.0056 (8)	0.0122 (8)	0.0067 (7)	0.0012 (8)	0.0001 (7)	-0.0007 (5)
N2	0.0103 (8)	0.0103 (7)	0.0056 (7)	-0.0002 (8)	-0.0003 (8)	-0.0019 (5)
Na1	0.0135 (4)	0.0164 (4)	0.0084 (4)	-0.0005 (4)	-0.0010 (4)	0.0027 (2)
O1	0.0089 (6)	0.0119 (6)	0.0082 (6)	0.0011 (7)	-0.0022 (7)	-0.0005 (4)
O2	0.0086 (7)	0.0214 (8)	0.0067 (6)	0.0002 (7)	0.0014 (6)	-0.0014 (5)
O3	0.0142 (8)	0.0329 (9)	0.0157 (8)	0.0120 (7)	-0.0030 (7)	-0.0045 (9)
O4	0.0142 (8)	0.0264 (8)	0.0197 (9)	-0.0095 (7)	0.0053 (7)	-0.0051 (7)
O5	0.0418 (10)	0.0106 (7)	0.0108 (6)	-0.0020 (9)	0.0036 (9)	-0.0012 (5)

Geometric parameters (\AA , $^\circ$)

C1—O2	1.259 (3)	N1—H1B	0.84 (3)
C1—O1	1.262 (2)	N1—H1C	0.91 (3)
C1—C2	1.526 (3)	N2—O4	1.241 (3)
C2—N1	1.489 (2)	N2—O3	1.242 (3)
C2—C3	1.528 (3)	N2—O5	1.264 (2)
C2—H2	0.94 (3)	N2—Na1	3.0312 (17)

C3—H3A	0.96 (3)	Na1—O1	2.3647 (13)
C3—H3B	0.97 (3)	Na1—O3	2.612 (2)
C3—H3C	1.00 (3)	Na1—O4	2.705 (2)
N1—H1A	0.92 (3)		
O2—C1—O1	123.16 (19)	C2—N1—H1C	110.9 (19)
O2—C1—C2	117.11 (17)	H1A—N1—H1C	108 (3)
O1—C1—C2	117.72 (17)	H1B—N1—H1C	106 (3)
N1—C2—C1	109.44 (16)	O4—N2—O3	121.22 (17)
N1—C2—C3	109.74 (16)	O4—N2—O5	119.3 (2)
C1—C2—C3	110.54 (17)	O3—N2—O5	119.5 (2)
N1—C2—H2	104.8 (17)	O4—N2—Na1	63.02 (11)
C1—C2—H2	109.2 (17)	O3—N2—Na1	58.74 (12)
C3—C2—H2	112.9 (17)	O5—N2—Na1	171.99 (11)
C2—C3—H3A	111.7 (17)	O1—Na1—O3	100.82 (6)
C2—C3—H3B	109.6 (18)	O1—Na1—O4	96.33 (6)
H3A—C3—H3B	108 (2)	O3—Na1—O4	47.99 (5)
C2—C3—H3C	115.1 (16)	O1—Na1—N2	102.85 (5)
H3A—C3—H3C	106 (2)	O3—Na1—N2	23.98 (6)
H3B—C3—H3C	106 (2)	O4—Na1—N2	24.14 (6)
C2—N1—H1A	110.8 (18)	C1—O1—Na1	137.35 (13)
C2—N1—H1B	112.4 (19)	N2—O3—Na1	97.28 (13)
H1A—N1—H1B	108 (3)	N2—O4—Na1	92.84 (13)

FT-IR study

In order to analyze the presence of functional groups, FTIR spectrum was recorded in the range of 400 cm^{-1} to 4000 cm^{-1} by using a MAGNO IR 750 series II NICOLET spectrometer. The samples were added to a matrix of KBr to perform this procedure. Fig. 5 shows the FTIR spectrum of p-LASN. Additionally on the same chart, the sample of pure L-Alanine is shown.

The presence of the carboxyl acid group around 3000 cm^{-1} can be observed due to the Alanine presence. Then, the main internal vibrations of Alanine are observed on the functional groups (NH_3^+ , CH_2 , COO^-) and this is in agreement with the data reported before [2] observing asymmetric vibrations on the NH_3 and CH_2 groups at 2987 cm^{-1} .

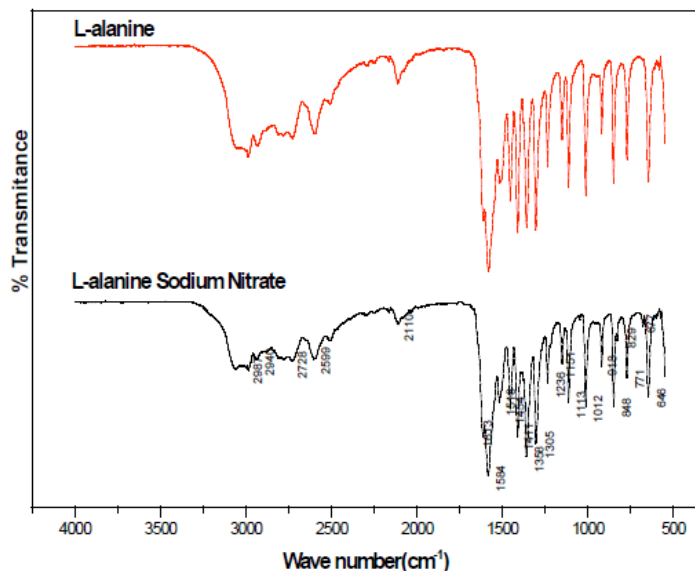


Fig. 5. FT-IR spectrum of Poly[μ_2 -L-alanine- μ_3 nitrate-sodium (I)] and L-Alanine reactive

The peak on 842 cm^{-1} is a symmetrical stretching NO_3 .

Also, the 1151 , 1218 and 1236 cm^{-1} are attributed to the rocking deformation of the NH_3^+ group [12]. Furthermore, the peak 1048 cm^{-1} is a symmetrical stretching of CCN group, too.

Other low frequency bands are typical for $\text{NH} \cdots \text{O}$ Hydrogen bonds arising from the overtones around the 2000 cm^{-1} .

The rest of the functional groups COO^- , CN and NO_3 between 500 and 1500 cm^{-1} also agree with the reported data.

Generally, the presence of nitrates in the lattice can be identified by their characteristic signature in the range of 1660 - 1625 , 1300 - 1255 , 870 - 833 and 763 - 690 cm^{-1} [9]. It is inevitable that the parent compound traces could also be identified in the synthesized compound. The presence of NO_3 group in the LASN can be identified by the peaks at 1350 , 1125 and 1055 cm^{-1} .

The symmetric and asymmetric NH_3^+ stretching vibrations appear at frequencies 3083 and 2937 cm^{-1} respectively. The C-H and N-H bending frequencies are observed at 1306 cm^{-1} . The absorption peaks at 1619, 1594, and 1508 cm^{-1} confirm the presence of NH_3 bending. The presence of nitro groups in the spectrum confirms the LASN compound. The laser Raman spectrum, showing the presence of more intense peak around 890 cm^{-1} , is due to COO stretching mode of vibrations (see Fig. 6). The less intense C-O-H bending mode vibrations are observed around 580 and 400 cm^{-1} . The peaks at 1350, 1125, and 1055 cm^{-1} are assigned to NO_3 stretching.

The C-H and N-H bending vibrations are observed at 1300 cm^{-1} as a sharp peak. The spectrum reported in Fig. 5 of Sethuraman et al. [3] shows asymmetric CH_3 bending at 1460 cm^{-1} and O-H bending is around 950 cm^{-1} . Rocking of O-H vibrations is observed at 1410 cm^{-1} [9]. In a crystalline powder groupings at the end of the faces of each crystal are free to change their polarizability, and hence peak intensity due to various groupings varies. Moreover, the intensity varies upon the source used for analyzing the sample.

Other important functional groups are detailed in Table 1.

Table 1. FT-IR Functional Group Assignments of the grown Poly[μ_2 -L-alanine- μ_3 -nitrate-sodium (I)]

Wavenumber (cm^{-1})	Assignments
2987	symmetric CH_3 stretching
2941	symmetric NH_3^+ stretching
2728	symmetric H-H...O and O-H...O stretching
2599	symmetric CH stretching
2511	overtone
2110	symmetric CH_3 stretching
1613	NH_3^+ bending
1584	NH_3^+ bending
1518	NH_3^+ bending
1454	asymmetric CH_3 bending
1411	symmetric C-COO stretching
1358	NO_3 stretching
1305	C-H and N-H bending
1236	NH_3^+ Rocking
1218	NH_3^+ Rocking
1151	NH_3^+ Rocking and symmetric CCOO stretching
1113	NO_3 stretching
1048	CCH Stretching
1012	Overtone of torsional oscillation of NH_3^+
918	Overtone of torsional oscillation of NH_3^+
848	NO_3 stretching
829	C-C Stretching
771	NO_3 stretching
677	overtone
646	COO in plane deformation
578	overtone

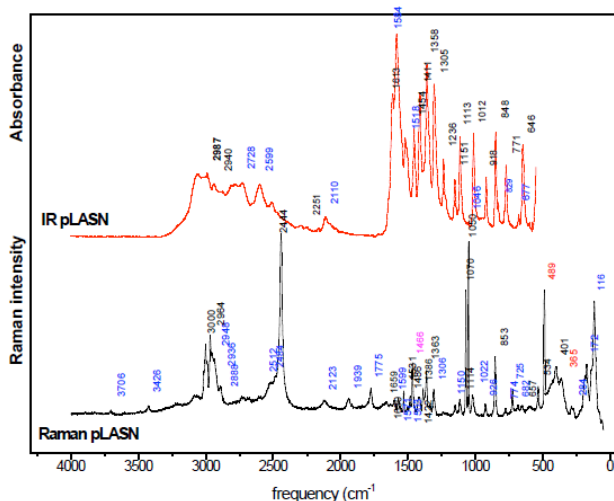


Fig. 6 Absorbance Raman and IR spectra showing the correspondence among some signals

UV- vis study

The UV-vis spectra give limited information about the structure of the molecule because the absorption of UV and visible light involves promotions of the electrons in the σ and π orbitals from the ground state to higher energy states. The transition spectra are very important for any NLO material because it can be of practical use only if it has a wide transparency window. NLO materials have a practical use only if they present a wide transparency state. To find this absorbance window, a Lambda 10 Perkin Elmer UV-Vis spectrometer was used. The scanning was done in the range of 200 to 1100 nm.

Same manner as the FTIR characterization, Fig. 7 shows the UV-Vis spectrum of the p-LASN plus the sample containing pure L-Alanine.

An absorbance zone behind 250 nm (Ultra-Violet wavelength) can be observed, showing also a wide band completely clear in all the visible range and even more (Infrared wavelengths) [2,3,8]. This means that this material presents a good non

absorbance band inside the visible range according to the desired situation due to the expected applications. It is important to observe a little protuberance around the 300 nm [4]. However, this little peak is still outside the visible zone (UV zone), and it could present some absorbance if the crystal would be excited with 600 nm (red color) trying to obtain a second harmonic of 300 nm (UV color). Other noticeable characteristic in the absorption spectrums is a wide transparency window within the range of 400–1100 nm which is desirable for NLO crystals because the absorptions in an NLO material near the fundamental or second harmonic signals will lead to the loss of the conversion of SHG. Due to this property, p-LASN has potential uses for SHG using a Nd:YAG laser (1064 nm) to emit a second harmonic signal within the green region (532 nm) of the electromagnetic spectrum. But GLiN is not a candidate for the third (355 nm) or fourth (266 nm) harmonics of Nd:YAG.

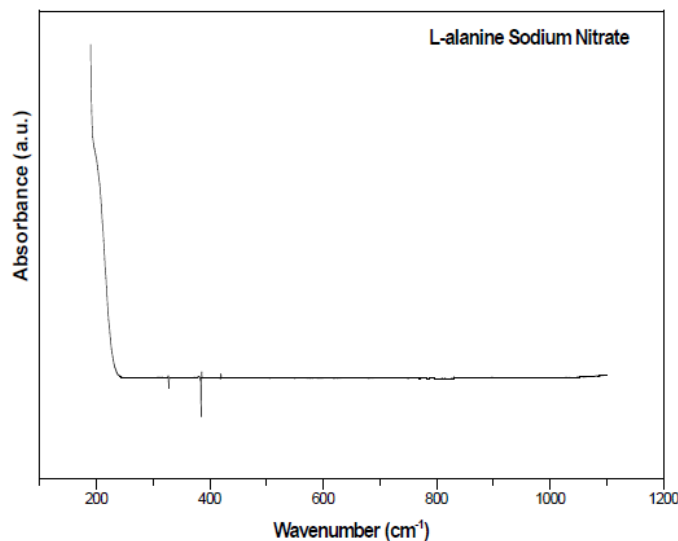


Fig. 7. UV-Vis-NIR de la muestra Poly[μ_2 -L-alanine- μ_3 -nitrate-sodium (I)]

Thermal analysis

TGA/DTA was done in a TA Instruments STD 2960 Simultaneous DTA-TGA. The samples were heated from room temperature to more than 1000° C at rate of 10° C/min.

Fig. 8 shows the TGA pattern of the p-LASN, showing a good stability below 220° C with a rapid dropping beyond that temperature [2,7].

In the same Figure also shows the DTA pattern of p-LASN where an exothermic transition appears at about 230° C. Meanwhile, the pure and presents another endothermic transition at 400° C [2,7].

Within this temperature range, the possible NLO applications become promising, due to the use of laser powers, observing a good performance below 230° C.

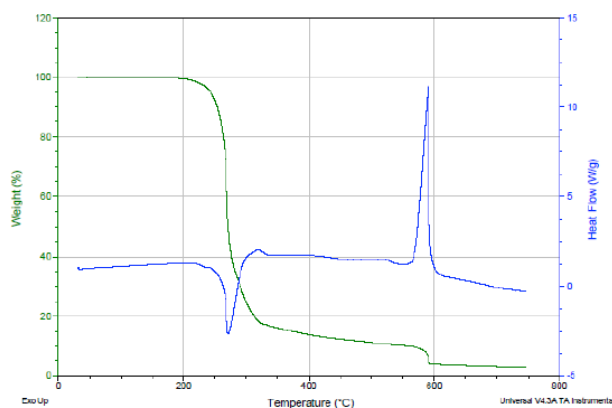


Fig. 8 TGA and DSC curves of Poly[μ_2 -L-alanine- μ_3 -nitrato-sodium (I)].

SHG signal detection

In order to find the SHG, the crystals was ground according to the Kurtz and Perry technique [2] into powder (about 70 μm) and densely packed between two transparent microscope glass slides [16,17]. Once the samples are placed into the glass slides, a Nd:YAG Quanta ray INDI series laser of 1064 nm, generating an 8 ns pulse and operated at 6 mJ/pulse and at rate of 10 Hz is pumped at the proper angle and

distance in order to see visibly the SHG on green color (532 nm); the expected emitted half wavelength signal.

The experimental array consists in a slightly modification to de Kurtz Perry method. A Nd:YAG pulsed laser source was the reference and excitation beam. The beam is divided in two beams consisting in a) reference beam and b) excitation beam. The reference beam is measured with a photomultiplier in order to detect the beam energy. The other one was used to exciting the sample, mounted between two glass holders. The emitting signal is after recorded in an oscilloscope in order to have the SHG intensity. Fig. 9 shows the experimental set.

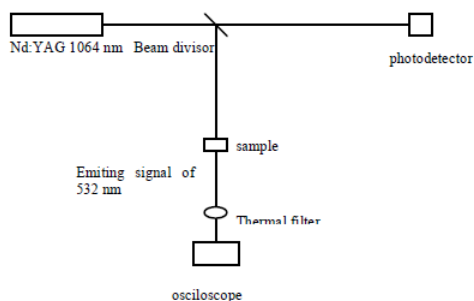


Fig. 9. Experimental set for SHG signal detection

Fig. 10 displays the data collected from the detector, where the SHG signal appears plotted vs the beam energy. This kind of experiments has been used in order to measure the damage threshold. In this case shows a tendency to increase the SHG intensity while the beam energy also is increased. With this experiment is noticeable the good second harmonic generation in this crystal.

Afterwards, the green emitted light was photographed in order to evidence the double frequency emission or SHG shown at the Fig. 11.

Showing the photograph at normal conditions in a computer monitor, the chromaticity was characterized applying a particular experiment design, using a PR-705 Spectroradiometer to analyze the color in terms of the CIE-1931 standard (See Fig.12).

Once the measurements were taken in different points, the averaged data was analyzed to obtain the dominant wavelength. This point at x and y obtained values are 0.2558 and 0.5617 respectively. The dominant wavelength is a point located on the saturated curve (the graph's edge). This point is obtained by tracing a straight line from the center point of the graph ($x = 0.3333$ and $y = 0.3333$), crossing through the measured point x and y and then, extend it until the saturation line, getting there the expected dominant wavelength, where the result was calculated by both methods (graphic and analytic).

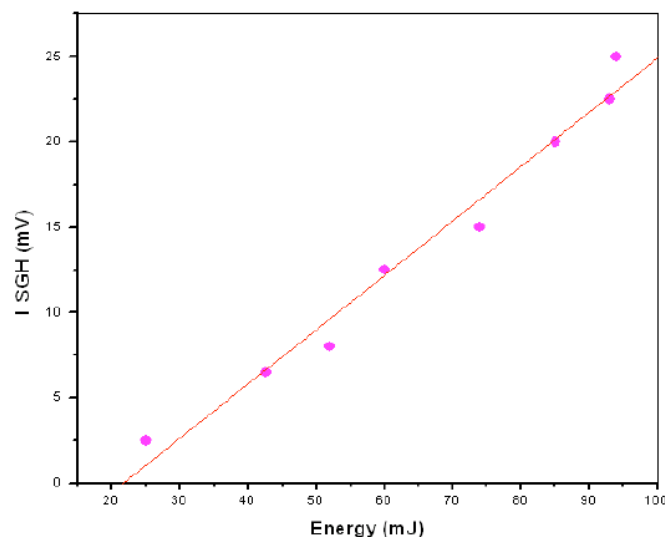


Fig. 10 Linear fit for the intensity of the SHG signal.

Then, It can be seen an obtained value of 533 nm that is to be the expected wavelength (green color 532 nm). This 1 nm difference among the obtained and expected data is possibly since this is a qualitative measurement, but it is not so

important due to the main purpose of this procedure that is in order to identify the Second Harmonic Generation in itself and not the perfect characterization of the emitted light so far. And also, it is important to consider that this procedure is fast and easy to apply in order to get confidence data.

Furthermore, taking advantage on the same equipment, the obtained luminance data helps to determine the efficiency of the samples. Luminance is the intensity by area unit (cd/m^2). Therefore, it depends on the emitted radiation through the measurement zone. In this particular case, this radiance comes from the computer monitor where the image was placed. Due to this situation, the obtained luminance data only can be used like relative values among different samples, not like absolutes. However, it is sufficient in order to detect which sample shows the best emission under SHG excitation and analysis in case of being a set of different samples to be analyzed.

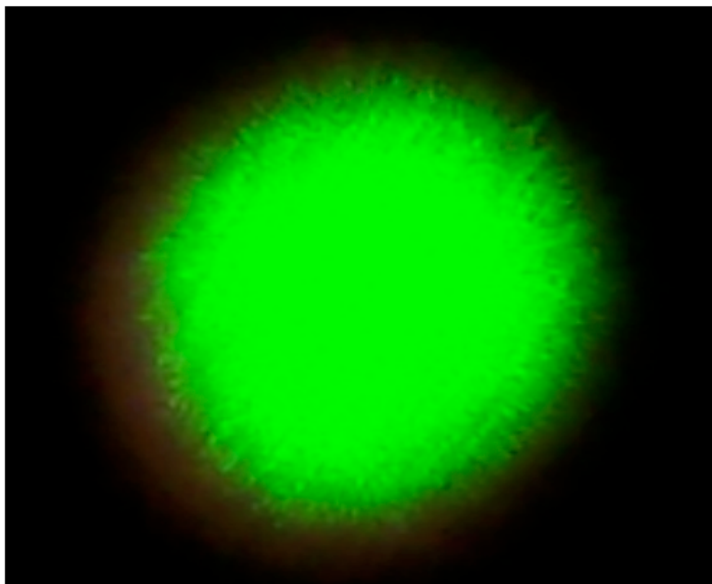


Fig. 11. Image of the SHG signal detected

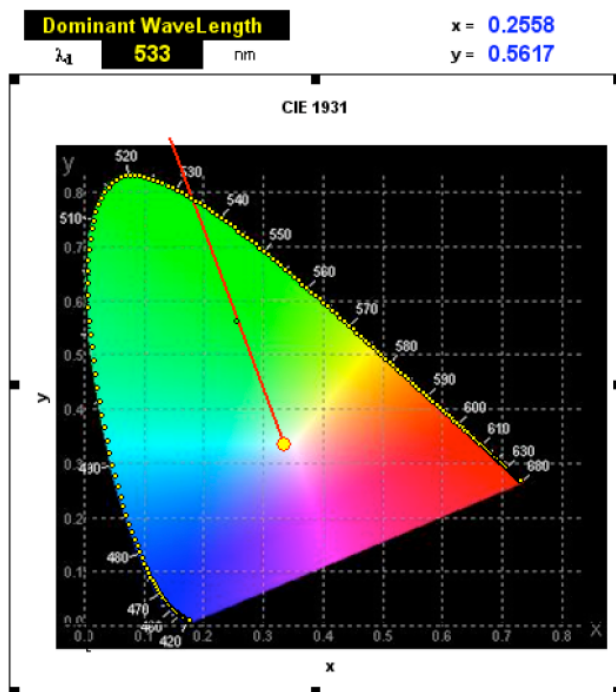


Fig. 12. Dominant wavelength of the SHG emission

Conclusion

A new non-linear optical semiorganic crystal Poly[μ 2-L-alanine- μ 3-nitrato-sodium (I)], p-LASN, was synthesized. The single crystals of p-LASN were grown from aqueous solution. The structure of p-LASN was confirmed by using the single crystal diffraction technique. It confirms that its lattice parameters are:

$$a = 5.388(9) \text{ \AA}, b = 9.315(15) \text{ \AA}, c = 13.63(2) \text{ \AA}, \\ \alpha = \beta = \gamma = 90^\circ$$

This unit cell was used to search the Cambridge Structural Databaseⁱⁱ (version 5.30 plus four updates). A positive match was found to the paper K. Van Hecke, E. Cartuyvels, T. N. Parac-Vogt, C. Gorller-Walrand, and L. Van Meervelt. Poly[μ 2-L-alanine- μ 3-nitrato-sodium(I)].

Was confirmed that the coordination geometry around the Na atom can be considered as trigonal–bipyramidal, with three bidentate nitrate anions coordinating through their O atoms and two l-alaninemolecules each coordinating through one carboxylate O atom.

Functional groups of good quality crystals of p-LASN grown by the slow evaporation technique, have been detected by FTIR and Raman spectroscopies.

Also, based on UV-vis spectra observations, an absorption zone under the 250 nm (Ultra-Violet wavelengths) can be seen, recovering a good transmittance values across all the visible range until near IR frequencies and beyond. This situation gives us the safety of applying this crystal for applications involving the band of visible light.

The tranparence nature of the crystal in the visible and infrared regions that form the transmission spectrum confirms the NLO property of the crystal.

Other characterization was the thermal response. In there, the TGA/DTA results show a degrading temperature about 230° C, which promises to have good applications at high temperatures, revealing that the crystal is thermally esable until that temperature.

The SHG test is the first one performed in this kind of material and we observe an important and strong dependence of the SHG intensity respect to the beam energy. Was imposible to detect de damage thresold because the intensity follows a linear tendence with a positive pendent, wich promise to be a good non-linear optical material.

Furthermore, color and intensity analysis were performed by a novel technique in order to verify the expected half dominant wavelength. In this point, the CIE-1931

chromaticity was used to locate the obtained color ($x = 0.2558$ and $y = 0.5617$). Then, aligning the CIE-1931 diagram's center point (white point) and the saturation line across the x and y measured point, a dominant wavelength of 533 nm is found, matching that it is very close to the expected emitted double frequency, translated in terms of wavelength of 532 nm.

Also, relative luminance values were measured in order to identify the possibility of analyzing different samples and therefore different SHG efficiencies among them. Finally we can conclude that we have obtained good quality crystals of Poly[μ 2-L-alanine- μ 3-nitrato-sodium (I)], pLASN, and we have detected as a first time the evidence of the second harmonic generation which indicates that pLASN is a new material with non-linear optical properties with potential applications.

Acknowledgments

The authors thank to the National Council of Science and Technology of Mexico for its financial support. Also to National Laboratory of Nanotechnology of CIMAV, S. C., at Chihuahua Mexico. The authors are very grateful to acknowledge to M. Sci. Enrique Torres Moye (Xray laboratory), M. Sci. Daniel Lardizabal (Thermal analysis laboratory), Luis de la Torre (Uv-vis analysis), Antonio Silva Molina (Raman study) and specially to Dr. Gary S. Nichols from the University of Arizona at Tucson for its technical support in the single crystal analysis.

References

- [1] N.Vijayan,S.Rajasekaran,G.Bhagavannarayana, R. Ramesh Babu, R. Gopalakrishnan, M. Palanichamy, and P. Ramasamy. Cryst. Growth Des, 2006, Vol 6, 11, 2441–2445.

- [2] M. Lydia Caroline, R. Sankar, R.M. Indirani, S. Vasudevan. *Materials Chemistry and Physics* 114 (2009) 490-494
- [3] S.A. Martin Britto Dhas, S. Natarajan. *Materials letters* 62 (2008) 2633-2636
- [4] M. Narayan Bhat, S. Dharmaprakash, *J. Cryst. Growth*. 236 (2002) 376–380.
- [5] C. Razzetti, M. Ardoino, L. Zanotti, M. Zha, C. Paorici, *Cryst. Res. Technol.* 37 (2002) 456– 465.
- [6] J.J. Rodrigues, L. Misoguti, F.D. Nunes, C.R. Mendonca, S.C. Zilo, *Opt. Mater.* 22 (2003) 235–240.
- [7] K. Ambujam, S. Selvakumar, D. Prem Anand, G. Mohamed, P. Sagayaraj, *Cryst. Res. Terchnol.* 41 (2006) 671–677.
- [8] G. Ramesh Kumar, S. Gokul Raj, R. Mohan, R. Jeyavel, *Cryst. Growth Des.* 6 (2006) 1308– 1310.
- [9] J. Baran, M. Drozd, A. Pietrazko, M. Trzebiatowska and H. Ratajczak. *Polish J. Chem.*, 77, 1561-1577 (2003)
- [10] D. Eimerl, S. Velsko, L. Davis, F. Wang, *Prog. Crystal Growth Charact.* 20 (1990) 59.
- [11] K.Sethuraman, R. Ramesh Babu, R. Gopalakrishnan, and P. Ramasamy. *Crystal Growth Des.* 8 (2008) 6, 1863-1869
- [12] Meera, K.; Muralidharan, R.; Dhanasekaran, R.; Prapun, M.; Ramasamy, P. J. *Cryst. Growth* 2004, 263, 510–516.
- [13] Mohankumar, R.; Rajanbabu, D.; Jayaraman, D.; Jayavel, R.; Kitamura, K. J. *Cryst. Growth* 2005, 275, e1935–e1939.
- [14] Narayan Bhat, M.; Dharmaprakash, S. M. J. *Cryst. Growth* 2002, 235, 511–516.

<https://cimav.repositorioinstitucional.mx/jspui/>

[15] Kristof Van Hecke, Els Cartuyvels, Tatjana N. Parac-Vogt, Christiane Goërrler-Walrand and Luc Van Meervelt. . Acta Crystallogr section E, 2007, 63, m2354

[16] S.K. Kurtz, T.T. Perry, J. Appl. Phys. 39 (1968) 3798–3813.

[17] Silverstein, R. M.; Webster F. X. Spectrometric Identification of Organic Compounds; 6th ed., John Wiley Eastern & Sons Inc.: Canada, 1998.

[18] N.Vijayan, R. Ramesh Babu, R.Gopalakrishnan, P. Ramasamy, W.T.A. Harrison, J. Cryst. Growth 262 (2004) 490-498.